

OBSERVATIONS AND MODELING OF FREQUENCY-DEPENDENT Lg CODA FROM PEACEFUL NUCLEAR EXPLOSIONS

Igor B. Morozov,¹ Hongyan Li,² Haishan Zheng,¹ and Scott B. Smithson²

University of Saskatchewan¹ and University of Wyoming²

Sponsored by Air Force Research Laboratory

Contract No. DTRA01-01-C-0057¹

ABSTRACT

Coda amplitude decay of regional arrivals from peaceful nuclear explosions (PNEs) could be used for characterization of crustal properties critical for seismic monitoring. In particular, as coda waves at 0.5–10 Hz are believed to predominantly consist of scattered shear waves, coda analysis could provide information about Lg attenuation and scattering from crustal heterogeneities. Digital recordings of 21 reversed PNEs, recorded by 200–400 three-component instruments within 0–3000 km range in northern Eurasia enable coda amplitude measurements to provide valuable information for understanding Lg propagation in the region. In this report, we focus on the analysis of the observed frequency dependence of Lg coda and ongoing efforts for its modeling.

A striking observation from comparative analysis of the PNEs is the difference of Lg coda decay characters across the study area. Within the East European Platform and south-west West Siberian Basin (profile QUARTZ), Lg coda amplitude decays exhibit clear frequency dependence that was previously described by frequency-dependent coda quality factor $Q \approx 350 f^{0.13}$ (f is the frequency). By contrast, within the Siberian Craton (profile KIMBERLITE), the coda exhibits a constant decay rate for all frequencies, which would correspond to Q nearly proportional to frequency. However, we argue that such a strong frequency dependence of Q could actually be due to a non-frequency-dependent coda attenuation process associated with geometric spreading and leakage of the energy from the crust (e.g., by refraction). The modified coda amplitude decay relation thus becomes

$$\frac{d \log A}{dt} \approx -\gamma - \frac{\pi f}{Q},$$

where γ is the coda geometric spreading factor. Notably, when using this form, γ remains constant ($\approx 0.003 \text{ s}^{-1}$) for the entire region, and $Q \approx 470$ for QUARTZ and $Q = \infty$ for KIMBERLITE. Very low attenuation within the Siberian Craton is also indicated by Pg propagating to unusual distances of 1600–1700 km. An additional advantage of using the above expression is that Q can now be viewed as frequency-independent.

Our modeling effort targets realistic, three-component phase amplitudes and codas produced by a distant PNE source. Currently, method and algorithm development and testing are underway. Simulations will be performed using a combination of three-dimensional (3D) visco-elastic finite-difference and 3D cylindrical screen propagator modeling. The finite-difference scheme will be utilized in the vicinities of the source and receivers, while the screen propagator will be used to propagate the energy to regional distances. The codes are parallelized using the Parallel Virtual Machine and implemented on two Beowulf clusters. Both codes are parts of an integrated seismic processing system, allowing tight integration of the models and providing a powerful user interface. When complete, this modeling package will provide the means for testing the above model of geometrical spreading and also to invert the Lg Q and Lg coda amplitude decay data for crustal attenuation.

OBJECTIVES

High-frequency regional phases used in CTBT monitoring (*Lg*, *Pg*, *Pn*, *Sn*) travel through the crust and the upper mantle and are therefore sensitive to the effects of these highly heterogeneous parts of the Earth. Large bodies of densely sampled observations and realistic modeling are required for understanding the properties of these phases and predicting their propagation across contrasting tectonic structures. In northern Eurasia, despite the paucity of its natural seismicity, such analysis is facilitated by the availability of dense regional phase recordings along the refraction lines of the Deep Seismic Sounding program, many of them using PNEs (Figure 1). In this project, we analyze PNE recordings for the purposes of regional seismic calibration. The general objectives of this study are as the following:

- 1) Gathering empirical data on amplitude and spectral characteristics of the regional phases in DSS PNE records, in their relation to the tectonic and geological structures.
- 2) Using numerical modeling, establishing semiempirical relationships between the in situ crustal properties and the observed wavefield characteristics. Among these characteristics, we are particularly interested in the quality factor, *Q*, describing attenuation of seismic waves.

In particular, in this report, we focus on observations and interpretation of frequency dependence of *Lg* coda *Q* and preliminary results of modeling aimed at elucidation of *Lg* coda *Q* properties.

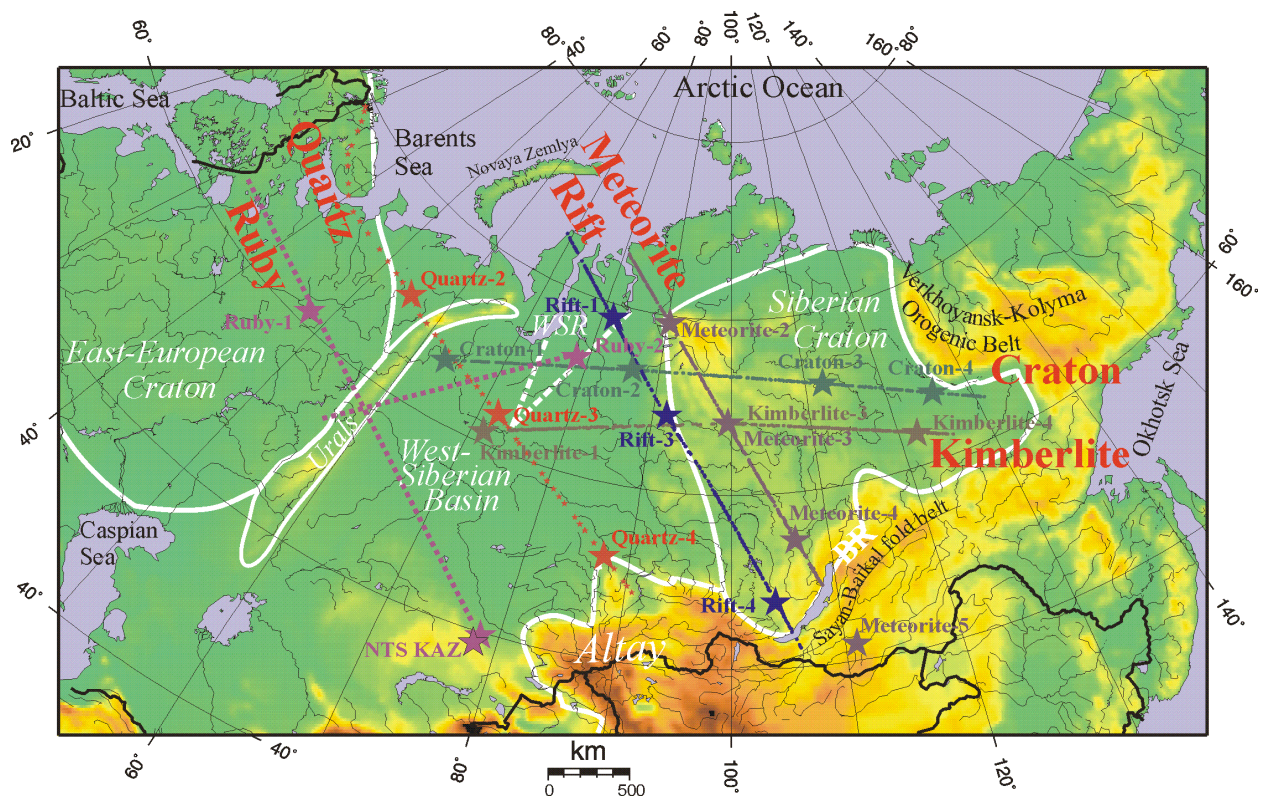


Figure 1. Location of PNE profiles used in this study shown on the background of topography of northern Eurasia. Large labeled stars indicate nuclear explosion locations, and small stars indicate the chemical explosions. For profile QUARTZ, small dots show chemical explosions; for other profiles, they show individual station locations. Two lines of project RUBY are shown schematically. White lines show major tectonic features (WSR, West Siberian Rift; BR, Baikal Rift), and color represents the topography (Zonenshain, 1990).

RESEARCH ACCOMPLISHED

Geometrical-spreading corrected vs. frequency-dependent coda Q

Measurements of the frequency-dependent quality factor, $Q(f)$, often results in Q increasing with frequency, which is conventionally expressed as a power law,

$$Q(f) = Q_0 \left(\frac{f}{f_0} \right)^\eta, \quad (1)$$

where f_0 is a reference frequency often taken equal 1 Hz. Both Q_0 and exponent η are assumed constant within the frequency range of interest, and thus relation (1) essentially represents fitting a two-parameter dependence to the observations of Q made at a set of selected frequencies. The power-law dependence appears to be generally dictated by convenience and represents a suitable parameterization in most cases. From several Lg Q and Lg coda Q studies, the frequency-dependence parameters η typically range from ~ 0.1 to near 1.0 (e.g., Nuttli, 1973; Mitchell, 1975; Frankel, 1991; Benz et al., 1997; Mitchell et al., 1997, 1998; McNamara, 2001; Erickson et al., 2004). General correlation to tectonics appears to suggest that active tectonic regions are characterized by low Q_0 and high η , while stable cratons are characterized by higher Q_0 and lower η (Erickson et al., 2004).

An initial attempt for application of the above conclusion to the region and frequency band of DSS profiles led to similar observations (Morozov and Smithson, 2000). Measurements of Lg coda Q at frequencies ~ 2 and 5 Hz from PNE QUARTZ-4 in the Mezenskaya Depression (near the position of PNE QUARTZ-2 in Figure 1) resulted in the values of $Q_1 = 350$ (at $f_0 = 1$ Hz) and $\eta = 0.13$ in relation (1) (Figure 2; Morozov and Smithson, 2000). The somewhat low Q_0 value was explained by the influence of thick sediments within the depression, and low η appears in agreement with the stable East European Platform.

Similar measurements using the records from profiles KIMBERLITE and METEORITE in Siberia lead to strikingly different results. From the unusual

efficiency of Pg propagation within the Siberian Craton, crustal Q was expected to be relatively high (Figure 3). In addition, travel-time modeling of QUARTZ profile (Figure 1) also suggested a simpler, layered crustal structure with little Moho topography within the West Siberian Basin as compared to the northern parts of the East European Platform (Shueller et al., 1997; Morozova et al., 1999). However, the logarithm of Lg coda amplitude measured from PNE KIMBERLITE-3 at a station within the Siberian craton shows an approximately frequency-independent decay (Figure 4). When interpreted in terms of the usual assumption of correctly compensated geometrical spreading of the coda (Morozov and Smithson, 2000), this decay is entirely due to the coda Q :

$$\log A_{coda}(f, t) = \text{const} - \frac{\pi f}{Q(f)} t = \text{const} - \frac{\pi}{Q_0} f^{1-\eta} t. \quad (2)$$

To account for the frequency-independent decay rate in relation (2), $Q(f)$ should be proportional to the frequency, corresponding to $\eta \approx 1$ in power law (1). Q_0 can be estimated as ~ 200 for Lg coda and 400 for the S-wave coda, both values appearing surprisingly low for this cratonic area and in disagreement with other observations.

The observations above suggest that the interpretation of the frequency dependence of Q could be reconsidered, at least for strong ($\eta \approx 1$) frequency dependences, in the DSS frequency band (~ 1 –10 Hz), or within the area of this

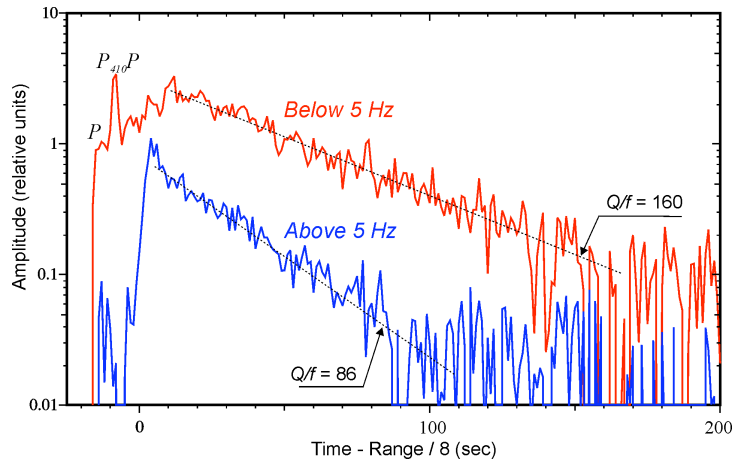


Figure 2. Amplitude-time decay for Lg coda from PNE QUARTZ-4, measured near the position of PNE QUARTZ-2 (Figure 1). Note the increasing amplitude decay rate with frequency; this increase is indicative of seismic attenuation. The Q/f values measured from the slopes are given in the labels.

study. Note that the strong frequency dependence of Q arising from formula (2) is observed for the entire KIMBERLITE profile (Figure 5) and not only at the location presented in Figure 4.

High $h \approx 1$ values in relation (1) imply that attenuation is quickly reduced with frequency. Liu et al. (1976) showed that linear visco-elastic rheology based on a “generalized standard linear solid” could explain frequency-dependent intrinsic attenuation observed during wave propagation through Earth materials. However, laboratory measurements are carried out at significantly higher frequencies and shorter wavelengths than those of the seismic waves considered here. At short-period seismic scales (100–10000 m), pervasive crustal and upper-mantle heterogeneity creates a complex interplay of numerous rheologies and could result in completely different properties. In particular, the presence of an attenuating component (e.g., water or small foids) would reduce the inferred high Q at higher frequencies. Moreover, for coda waves bouncing within the crustal waveguide, scattering should be the primary contributor to their attenuation. For scattering, attenuation decreasing with frequency would mean that the total volume of scatterers drops nearly linearly at smaller scale lengths. Although this could be possible, it still appears unlikely that heterogeneities within the West Siberian Basin and Siberian Craton become progressively less abundant as their sizes reduce. Typically, scaling laws suggest increasing representation of heterogeneities (e.g., faults and topographic features) at smaller scales.

Accepting the above conjecture that high h could in fact be observed where Q is very high, we note that the frequency-independent amplitude decay should not be related to the attenuation defined as an energy dissipation process proportional to the number of wave cycles (that is, to $f t$). Instead, if coda amplitude decay with time includes a purely geometrical component, it could be approximated by the following relation:

$$\log A_{coda}(f, t) = \text{const} - \left(\gamma + \frac{\pi f}{Q} \right) t \quad (3)$$

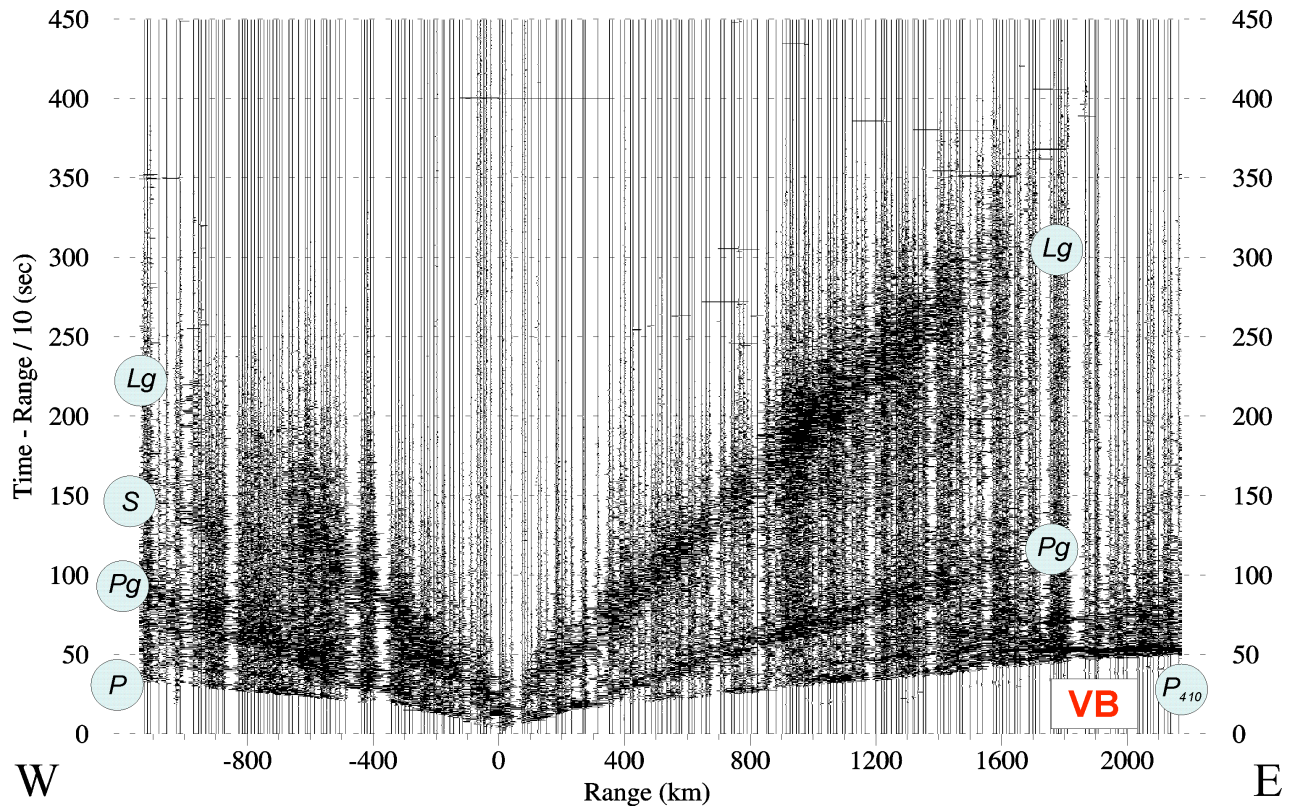


Figure 3. Vertical-component records from PNE CRATON-2 (Figure 1). Note the unusually strong propagation of Pg to ~1700 km from the shot, quickly attenuating within the Viluy basin (VB). Such high propagation efficiency suggests high crustal Q , at least in the eastern part of the profile.

Here, γ describes an effective geometrical spreading process. Amplitude decaying with scattering time and independent of the frequency could correspond, for example, to leaking of the wave energy out of the Pg/Lg waveguide as the multiple-reflected waves bounce within it (Gutenberg, 1955). Note that the exponential relation for $A_{\text{coda}} \propto \exp(-\gamma t)$ is primarily dictated by the convenience of working in the $(t, \log A)$ plane. With significant measurement errors inherent in attenuation measurements, other frequency-independent expressions could be defined, yet in practice, they could hardly be distinguished from form (3).

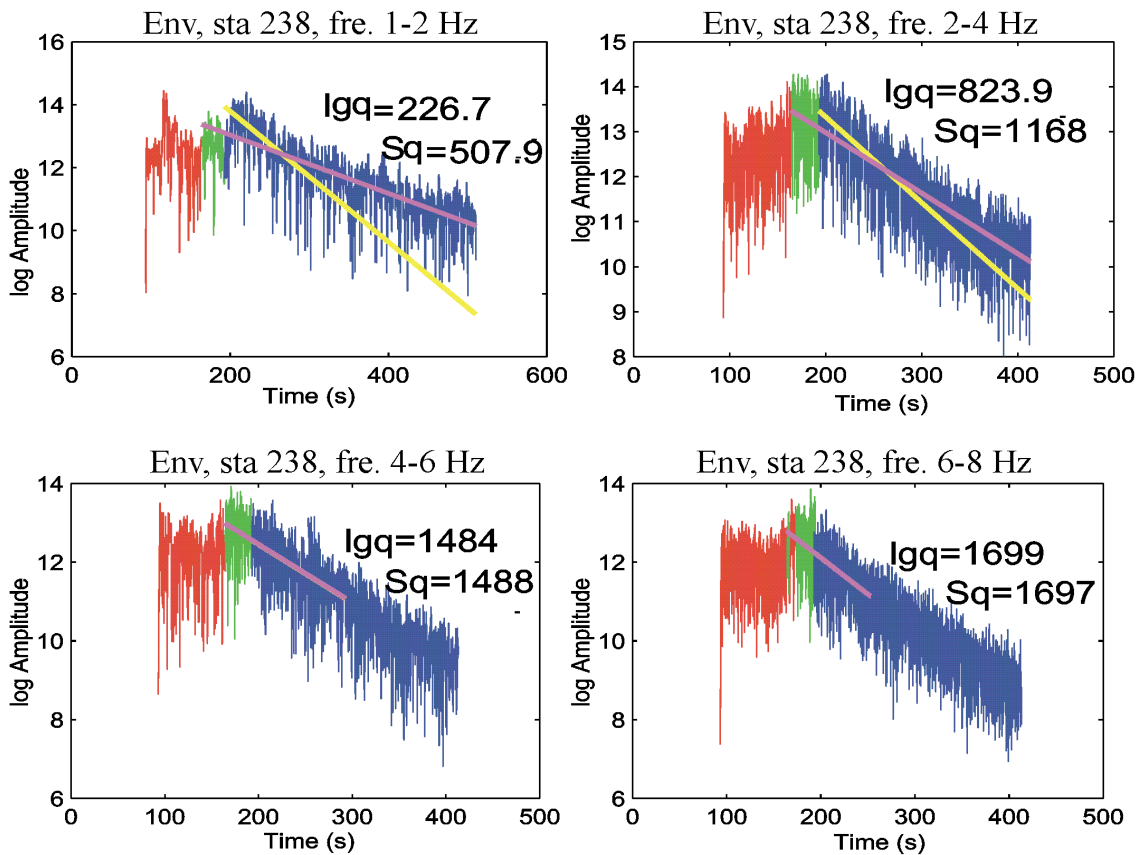


Figure 4. Amplitude envelope of vertical-component record from station 238 from PNE KIMBERLIE-3 filtered within frequency bands of 1–2, 2–4, 4–6, and 6–8 Hz (labeled). Estimated coda Q for the S-wave and Lg coda windows are indicated. Note that these Q values quickly increase with frequency. Also note that at the same time, temporal slopes of log (amplitudes) appear to be independent on the frequency bands.

With a single constant Q , expression (3) represents another two-parameter relation for $\log A_{\text{coda}}(f, t)$, which is an alternative to (2). Although Q could also be theoretically considered as frequency-dependent in formula (3), distinguishing this dependence from the effect of γ appears highly problematic with the available data. Thus, in a minimalistic approach, we view the form (3) with a single and constant Q as a viable alternative to frequency-dependent $Q(f)$ for the DSS PNE data. Potential extrapolation of this conjecture to other situations will still need to be examined in the future.

Within the accuracy of fitting relations (2) or (3) to the typical data, both of them apparently could be used interchangeably. Thus, the dependence (3) with $Q = \tilde{Q}$, when recast in the form (2), would lead to frequency-dependent attenuation with

$$\eta = -\log_f \left(\frac{\gamma}{f_{ref}} + \frac{\pi}{\bar{Q}} \right), \quad (4)$$

where the reference frequency f_{ref} could be selected within the frequency band. This shows that $\eta = 0$ for $\gamma = 0$ and $\eta \rightarrow 1$ when $Q \rightarrow \infty$. A high γ (steep geometrical coda amplitude decay, as possibly caused by strong crustal folding and rough Moho) would thus explain the low Q_0 and high η observed in active tectonic areas.

Using the dependence (3) instead of (2) to fit QUARTZ-4 (Figure 2) and KIMBERLITE-3 (Figure 4) observations reveals that, for both datasets, the geometrical factor is the same, $\gamma \approx 0.003 \text{ s}^{-1}$, with $Q \approx 470$ for QUARTZ and $Q = \infty$ for KIMBERLITE. In agreement with the observations of unusually efficiently propagating P_g within the Siberian Craton, its crust shows very low attenuation. Close geometrical factors both east and west of the Uralian belt (Figure 1) could also be expected, as crustal structure remains generally similar on both sides. As another hypothesis, it appears that crustal thickness could be the primary factor controlling the values of γ . With increasing crustal thickness, the number of reverberations required to form a crustal-guided phase at a given distance would decrease, leading to lower values of geometrical attenuation γ .

If confirmed by further analysis of the DSS PNE and other data, the above observations could have several important implications for seismic calibration and nuclear test monitoring. First, as frequency dependence of Q trades off with geometrical spreading, it is important to eliminate this uncertainty before correlating the resulting parameters with the geological structures or looking for portable attributes. Equation (3) removes this trade-off by defining the geometrical spreading as a frequency-independent part of signal attenuation with time (distance). This could allow local measurements of geometrical spreading by spectral analysis of coda waves. The resulting spreading parameter γ could be regionalized and correlated with geology.

The second potential advantage from using form (3) arises from the stability of the geometrical exponent γ suggested by the present observations. If γ is confirmed to be stable or correlated with the crustal thickness, it could be used as a useful and transportable calibration parameter. Robust regional values of geometrical spreading could be utilized to correct the observed coda Q values. Moreover, because of their frequency independence, the resultant coda Q values also may have a better chance of being transportable between different frequency bands, types of observations, and geographic regions.

In most practical cases, removal of the $\gamma \leftrightarrow Q(f)$ trade-off would leave us with only frequency-independent Q in relation (3). The advantage of this point of view would be in freeing Q measurements from reliance on independent determinations of geometrical spreading, which are the critical part of most attenuation measurements (Benz et al., 1997). Note that because of their using band-limited data without explicitly enforcing frequency-independence, geometrical spreading estimates may also turn out to be effectively dependent on the frequency. In addition, (γ, Q) parameterization is also closer to and should be consistent with attenuation measurements using spectral ratio

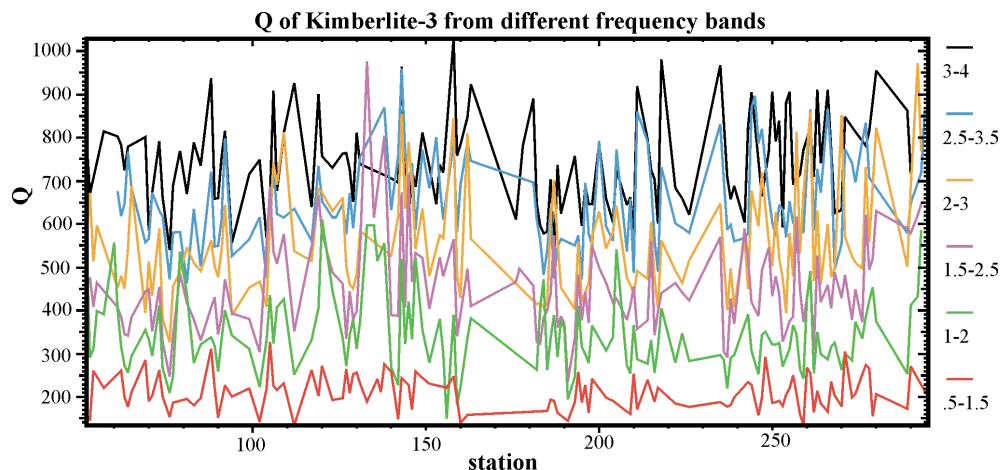


Figure 5. L_g coda Q of PNE KIMBERLITE-3 measured across the profile within several frequency bands (labeled on the right). Despite the scatter in the L_g Q values, Q consistently increases with frequency.

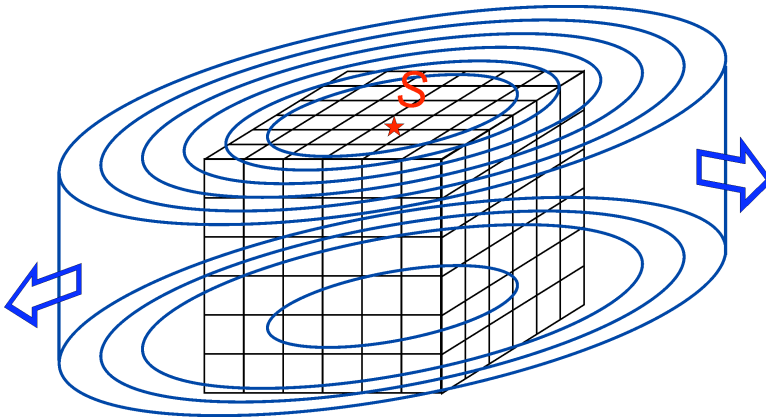


Figure 6. Schematic illustration of our 3D numerical wavefield simulation scheme. First, in the near-source region, the wavefield is modeled using a 3D visco-elastic finite-difference simulator (cubic grid). This field is propagated to regional distances using a modification of the Generalized Complex Screen Propagator method (blue cylindrical surfaces; Wu, et al., 2000).

techniques (which eliminate the absolute amplitude effects and rely on spectral slopes, thereby typically also producing frequency-independent Q estimates insensitive to the geometrical spreading).

Lg and coda modeling in 3D

Modeling short-period seismic phases in realistic crustal structures at regional distances is another key component of this project. Code development is still in progress, and here we only summarize the key ideas of the approach. We utilize parallel cluster computer systems (10- and 66-processor) to implement a hybrid 3D finite-difference (FD) and finite-element (FE) modeling scheme (Figure 6).

The near-source region is modeled using a parallel visco-elastic finite difference program based on the fourth-order finite-differencing scheme by Bohlen (2002). Compared with Bohlen's code, we use a different parallelization scheme (the Parallel Virtual Machine instead of the Message Passing Interface), an extensive user interface allowing us to build complexly structured models, more general periodic boundary conditions, and free-surface boundary conditions with arbitrary topography. The code has been integrated into our seismic processing system (Morozov and Smithson, 1997; Chubak and Morozov, in review), adding many options for user interaction with the code and for data and model visualizations.

Farther away from the source, full 3D FD simulations become impractical because of excessive demand on computational resources, and we switch to an efficient Generalized Screen Propagator (GSP) scheme first developed by Wu et al. (2000). However, unlike the original two-dimensional (2D) implementation (Wu et al., 2000, and references therein), we introduce the following new requirements to our screen propagator: (1) it should operate in 3D, and therefore the screens become cylindrical (Figure 6); (2) surface topography, the Moho depth, and the key crustal boundaries (such as the top of the basement) are explicitly included in the model and are allowed to vary; and (3) we allow for arbitrary velocity/density variations with depth and also their slow variations with propagation radius. This GSP scheme is therefore fundamentally different from that by Wu et al. (2000) and requires a different implementation. Owing to the structural complexity of the model, the finite element (FE) method apparently represents the most suitable approach to responding to the above requirements.

The FE scheme is formulated as follows. In variational formulation (see Aki and Richards, 2002, Chapter 7.3), solution of the wave propagation problem is reduced to finding a stationary point of a functional sometimes called Action,

$$A[\mathbf{u}] = \int d^3r L(\dot{\mathbf{u}}, \mathbf{u}), \quad (5)$$

where \mathbf{u} is the displacement field, the dot denotes the time derivative, and the Lagrangian $L()$ is the difference of the kinetic and potential energy densities. For an isotropic medium,

$$L(\dot{\mathbf{u}}, \mathbf{u}) = \frac{1}{2} \rho \dot{u}_i \dot{u}_i - \left[\frac{1}{2} \lambda (\varepsilon_{ii})^2 + \mu \varepsilon_{ij} \varepsilon_{ij} \right], \quad (6)$$

where ε is the strain tensor. Because the model is independent of the time variable, different Fourier harmonics do not interfere with each other, and in the frequency domain, (6) becomes

$$L(\dot{\mathbf{u}}, \mathbf{u}) = -\frac{\omega^2}{2} \rho u_i u_i - \left[\frac{1}{2} \lambda (\varepsilon_{ii})^2 + \mu \varepsilon_{ij} \varepsilon_{ij} \right]. \quad (7)$$

The problem reduces to maximization of the integral (5) by finding the appropriate spatial distribution of \mathbf{u} for each frequency ω . The Rayleigh-Ritz method achieves this by first approximating the wavefield by a linear combination of basis functions,

$$\mathbf{u}(\mathbf{r}) = c_i \boldsymbol{\theta}_i(\mathbf{r}). \quad (8)$$

The basis functions are chosen to satisfy the boundary conditions (zero normal traction at the free surface and radiation condition at the bottom of the model). In our case, for each screen, we associate the basis functions with a grid of points in depth, z , and azimuth, θ , so that

$$\boldsymbol{\theta}_{k,n,l} = J_0(kr) s_n(z) s_l(\theta), \quad (9)$$

where k is the radial wavenumber, J_0 is the zero-order Bessel function, and $s()$ are linear spline functions centered at node (n, l) respectively in the (z, θ) cylindrical surface. With the use of functional basis (8), action (5) becomes a quadratic form,

$$A[\mathbf{u}] = c_i A_{ij} c_j, \quad (10)$$

where A_{ij} is a sparse and symmetrical matrix. The key assumption of this GSP method, as with the method by Wu et al. (2000), is the preservation of the wavenumber between the screens (matrix A is thus approximately diagonal in k), so that, along with ω , k could be considered an integral of motion during the maximization. This approximation reduces the set of unknowns to one two-dimensional (2D) grid per screen, and the screens can be spaced relatively sparsely, making numerical maximization of (5) a tractable problem. The resulting matrix problem (10) can be solved by an iterative technique, such as conjugate gradients or LSQR. Because of the independent spoliations with different (ω, k) , the method can be parallelized in a straightforward manner.

CONCLUSIONS AND RECOMMENDATIONS

Analysis of the frequency-dependent Lg coda Q from several DSS PNE profiles in northern Eurasia indicates significant differences in attenuation properties between the East European Platform and the West Siberian Basin and the Siberian Craton. A consistent interpretation arises from abandoning the traditional $Q(f) = Q_0 f^\gamma$ model in favor of the model utilizing regionally-variable geometrical spreading and frequency-independent attenuation. In this model, the geometrical spreading is consistent between the two studied areas, and the attenuation appears to be very low within the Siberian Craton, in agreement with other observations.

If confirmed by further analysis, these observations could have several important implications for seismic calibration and nuclear test monitoring:

- 1) It would allow more consistent and reliable measurements of geometrical spreading and Q .
- 2) The geometrical exponent γ is likely to be stable or correlated with the crustal thickness, in which cases it could be used as a useful and transportable calibration parameter.
- 3) Because of their frequency independence, the resultant coda Q values also may also be better transportable between different the frequency bands, types of observations, and geographic regions.

In numerical modeling, we described a comprehensive hybrid parallel 3D finite-difference and finite-element screen propagator method that should allow simulations of short-period wavefields to regional distances, with an account of

27th Seismic Research Review: Ground-Based Nuclear Explosion Monitoring Technologies

the topography of the free surface, of the Moho, and of the key intracrustal boundaries. The method should also be able to handle depth and lateral velocity variations. Finally, the method is currently being implemented in an integrated seismic processing package that will provide uniform model parameterization, input/output, and visualization.

REFERENCES

- Aki, K. and P. G. Richards (2002), *Quantitative Seismology*, 2nd Ed. Sausalito, CA: University Science Books.
- Benz, H., A. Frankel, and D. Boore (1997), Regional *Lg* Attenuation in the Continental United States, *Bull. Seism. Soc. Am.* 87: 600–619.
- Bohlen, T. (2002), Parallel 3-D Viscoelastic Finite Difference Seismic Modelling, *Comput. Geosciences* 28: 887–899.
- Chubak, G. and I. B. Morozov, (in review), Integrated Software Framework for Processing of Geophysical Data, *Comput. Geosciences*.
- Erickson, D., D. E. McNamara, and H. Benz (2005), Frequency-Dependent *Lg Q* within the Continental United States, *Bull. Seism. Soc. Am.* 94: 1630–1643.
- Frankel, A. (1991), Mechanism of Seismic Attenuation in the Crust: Scattering and Inelasticity in New York State, South Africa, and Southern California, *J. Geophys. Res.* 96: 17441–17457.
- Gutenberg, B. (1955), Channel Waves within Earth's Crust, *Geophysics* 20: 283–294.
- Liu, H. P., D. L. Anderson, and H. Kamamori (1976), Velocity Dispersion due to Anelasticity: Implications for Seismology and Mantle Composition, *Geoph. J. Roy. Astr. Soc.* 47: 41–58.
- McNamara, D. E. (2000), Frequency-Dependent *Lg* Attenuation in South-Central Alaska, *Geophys. Res. Lett.* 27: 3949–3952.
- Mitchell, B. (1975), Regional Rayleigh Wave Attenuation in North America, *J. Geophys. Res.* 80: 4904–4916.
- Mitchell, B. J. and L. Cong (1998), *Lg* coda *Q* and Its Relation to the Structure and Evolution of Continents: A Global Perspective, *Pure Appl. Geophys.* 153: 655–663.
- Mitchell, B. J., Y. Pan, J. Xie, and L. Cong (1997), *Lg* Coda *Q* Variation across Eurasia and Its Relation to Crustal Evolution, *J. Geophys. Res.* 102: 22767–22779.
- Morozov, I. B., and S. B. Smithson (2000), Coda of Long-Range Arrivals from Nuclear Explosions, *Bull. Seism. Soc. Am.* 90: 929–939.
- Morozov, I. B. and S. B. Smithson, (1997), A New System for Multicomponent Seismic Processing, *Comput. Geosciences* 23: 689–696.
- Morozova, E. A., I. B. Morozov, S. B. Smithson, and L. N. Solodilov (1999), Heterogeneity of the Uppermost Mantle beneath the Ultra-Long Range Profile “Quartz,” Russian Eurasia, *J. Geophys. Res.* 104 (B9): 20, 329–330, 348.
- Nuttli, O. (1973), Seismic Wave Attenuation and Magnitude Relations for Eastern North America, *J. Geophys. Res.* 78: 87–885.
- Schueller, W., I. B. Morozov, and S. B. Smithson (1997), Crustal and Uppermost Mantle Velocity Structure of Northern Eurasia along the Profile Quartz, *Bull. Seism. Soc. Am.* 87: 414–426.
- Wu, R.-S., S. Jin, and X.-B. Xie (2000), Energy Partition and Attenuation of *Lg* Waves by Numerical Simulation Using Screen Propagators, *Phys. Earth. Planet. Inter.* 120: 227–243.
- Zonenshain L. P., M. I. Kuzmin, and B. M. Natapov (1990), *Geology of the USSR: A Plate Tectonic Synthesis*. Washington, DC: American Geophysical Union.